DOI: 10.1002/chem.200800470

Ruthenium-Based Olefin Metathesis Catalysts Coordinated with Unsymmetrical N-Heterocyclic Carbene Ligands: Synthesis, Structure, and Catalytic Activity

Georgios C. Vougioukalakis and Robert H. Grubbs*[a]

Abstract: A series of ruthenium-based olefin metathesis catalysts coordinated with unsymmetrical N-heterocyclic carbene (NHC) ligands has been prepared and fully characterized. These complexes are readily accessible in one or two steps from commercially available $[(PCy_3)_2Cl_2Ru{=}CHPh]$. All of the complexes reported herein promote the ring-closing of diethyldiallyl and diethylallylmethallyl malonate, the ring-opening metathesis polymerization of 1,5-cyclooctadiene, and the cross metathesis of allyl benzene with *cis*-1,4-diacetoxy-2-butene, in some cases surpassing in efficiency the existing second-generation catalysts. Especially in the cross metathesis of allyl benzene with *cis*-1,4-diacetoxy-2-butene, all new catalysts demonstrate similar or higher activity than the second-generation ruthenium catalysts and, most importantly, afford improved *E*/*Z* ratios of the desired cross-product at conversion above 60%. The influence of the unsymmetrical NHC ligands on the initiation rate and the activation parameters for the irreversible reaction of these ruthenium complexes with butyl vinyl ether were also studied. Finally, the synthesis of the related chlorodicarbonyl(carbene) rhodium(I) complexes allowed for the study of the electronic properties of the new unsymmetrical NHC ligands that are discussed in detail.

Keywords: carbene ligands · homogeneous catalysis · olefin metathesis · rhodium · ruthenium

Introduction

The development of ruthenium-based metathesis catalysts with high air and moisture stability and functional-group tolerance has led to the use of olefin metathesis, one of the most powerful carbon–carbon bond-forming reactions,[1] in a variety of applications in organic synthesis and polymer chemistry.[2] The synthesis of the first well-defined ruthenium olefin metathesis initiator (**1**) was published in 1992.[3] However, this early catalyst was only effective in the ring-opening metathesis polymerization (ROMP) of highly strained olefins. Although the basic structure of the currently used ruthenium-based catalysts still resembles that of the original complex, comprised of a ruthenium alkylidene, two halides, and two neutral ligands, contemporary catalysts (**2–5**) are much more robust and functional-group tolerant. For example, the first-generation catalyst **2** has much better functional group compatibility than all of the early-transition-metal olefin metathesis initiators.[4] Replacement of one of the tricyclohexylphosphine ligands with the bulky N-heterocyclic carbene (NHC) ligand H_2IMes produced ruthenium complex **3**, which displays improved catalytic activity, while maintaining the high functional group tolerance and

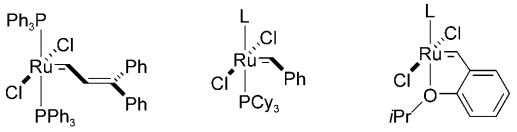

1 **2** L = PCy_3 **4** L = PCy_3

3 L = H_2IMes **5** L = H_2IMes

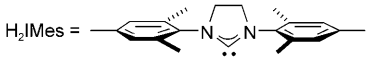

[a] Dr. G. C. Vougioukalakis, Prof. Dr. R. H. Grubbs
Arnold and Mabel Beckman Laboratory of Chemical Synthesis
Division of Chemistry and Chemical Engineering
California Institute of Technology
1200 East California Blvd, Pasadena, CA 91125 (USA)
Fax: (+1) 626-564-9297
E-mail: rhg@caltech.edu

Supporting information for this article is available on the WWW under http://dx.doi.org/10.1002/chem.200800470. It contains ^{1}H, ^{13}C, ^{19}F, and ^{31}P NMR spectra of catalysts **8–13**, plots with additional catalytic evaluation data for **6–13**, initiation kinetics plots and tables for catalysts **6–13**, and IR spectra for Rh complexes **29–33**.

thermal stability of **2**.[5] Furthermore, substitution of the phosphine ligands for bidentate carbenes (complexes **4** and **5**) led to ruthenium-based metathesis catalysts with even higher thermal stability.[6] More recent studies have fostered the development of ruthenium-based catalysts that initiate asymmetric olefin metathesis reactions,[7] and have led to metathesis applications in aqueous and protic solvent systems,[8] and the challenging formation of tetrasubstituted carbon–carbon double bonds.[9]

Unsymmetrically substituted five-membered NHCs, namely having two different exocyclic substituents adjacent to the carbenic center, have also been successfully utilized as ligands in ruthenium metathesis catalysts.[7b–e,10–17] Other unsymmetrical carbenic frameworks that have been recently incorporated in ruthenium-based catalysts include a series of cyclic(alkyl)(amino) carbenes,[18] and thiazole-2-ylidenes.[19] Unsymmetrical NHC frameworks, especially those with an aliphatic amino side group, were initially used in order to increase the electron-donating ability of the NHCs and, therefore, enhance the catalytic activity of the corresponding complexes.[11,13,16] Additionally, it has been found that the utilization of unsymmetrical NHCs alters the selectivity in diastereoselective ring-closing metathesis (RCM) reactions and the *E*/*Z* selectivity in cross-metathesis (CM) reactions.[12,15,17]

Building upon our preliminary studies on the development of unsymmetrical catalysts **6** and **7**, bearing an NHC that has one mesityl and one 2,6-difluorophenyl group,[15] we

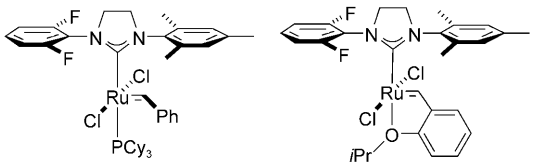

6 **7**

now report the synthesis and catalytic evaluation of unsymmetrical catalysts **8–13**. These catalysts were fully characterized, and their catalytic performance was evaluated in RCM, ROMP, and CM reactions. Some complexes were found to surpass the commercially available second-generation catalysts in efficiency. Moreover, in the CM of allyl benzene with *cis*-1,4-diacetoxy-2-butene, catalysts **8–13** provide improved *E*/*Z* selectivity of the desired cross-product at conversions higher than 60%. The initiation rates and the activation parameters in the irreversible reaction of catalysts **8–13** with butyl vinyl ether were also studied. The rate-limiting step for the initiation of all phosphine-containing catalysts was found to be phosphine dissociation. The kinetics in the initiation of the phosphine-free catalysts are more complicated; however, the related experiments suggest that oxygen dissociation is not rate-determining. The electron-donating ability of the new unsymmetrical NHCs was finally studied in the rhodium(I) complexes of the general formula $[Rh(CO)_2Cl(NHC)]$ by using FT-IR spectroscopy. The synthesis of these rhodium(I) complexes was carried out by transmetalation from the corresponding Ag(I) complexes.

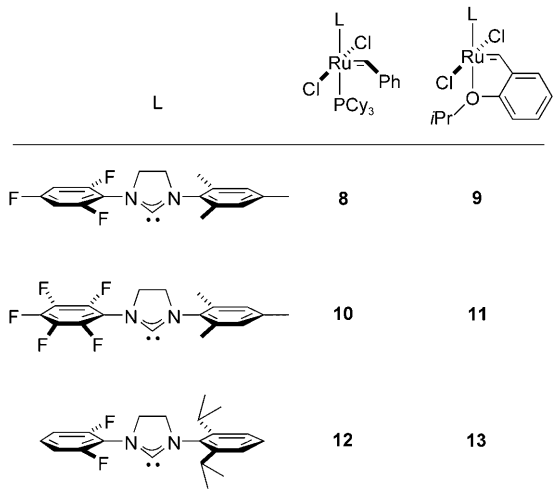

L		
	8	**9**
	10	**11**
	12	**13**

Results and Discussion

Synthesis and characterization of the new ruthenium complexes: The synthesis of carbene precursors **18a–c** is straightforward (Scheme 1), following a modification of previously reported procedures.[15,20] The appropriate anilines

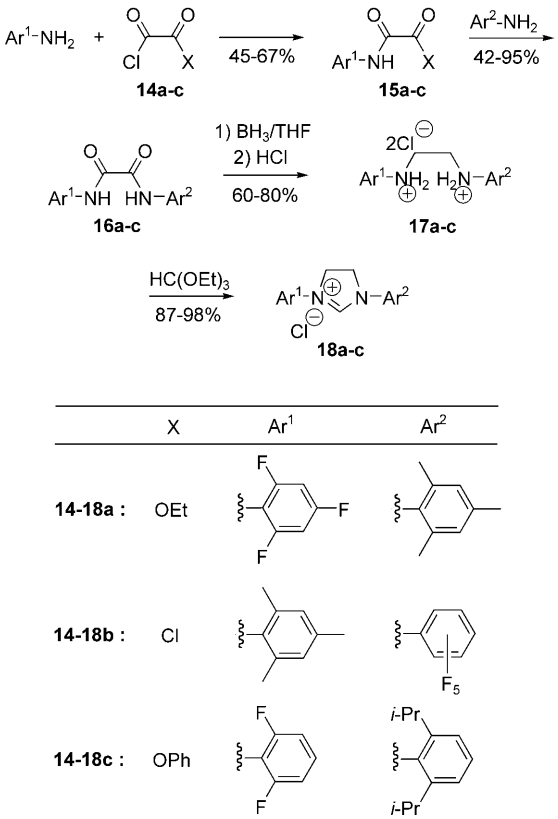

	X	Ar^1	Ar^2
14-18a :	OEt		
14-18b :	Cl		
14-18c :	OPh		

Scheme 1. Synthesis of 4,5-dihydroimidazolium chlorides **18a–c**.

were initially treated with oxalyl chloride, ethylchlorooxoacetate, or phenylchlorooxoacetate (**14a–c**) to afford the corresponding condensation products **15a–c**. Upon addition of the second aniline, oxalamides **16a–c** were isolated. These were reduced with BH_3·THF and then treated with HCl to furnish dihydrochloride salts **17a–c** that, upon treatment with triethyl orthoformate, cyclize to imidazolinium chlorides **18a–c**. Complexes **8**, **10**, and **12** were isolated in 46–80% yield by generation of the free carbene from **18a–c**, in situ with potassium hexamethyldisilazane (KHMDS), and then reacted with ruthenium source **2** in benzene. Treatment of **8**, **10**, and **12** with *o*-isopropoxy-β-methylstyrene afforded the phosphine-free analogues **9**, **11**, and **13** in 57–85% yield. Compounds **8–13** are air stable in the solid state and can be purified by silica gel chromatography.

Complexes **8–13** were completely characterized by NMR spectroscopy and HRMS (see the Supporting Information). Even at temperatures as low as −70 °C, the NHCs of complexes **9**, **11**, and **13** rotate fast on the NMR timescale and, therefore, only one absorption is observed in the benzylidene region of the ^{1}H NMR spectra (around 16 ppm) for these phosphine-free complexes. In contrast, phosphine-containing complexes **8**, **10**, and **12**, in solution, are a mixture of two rotational isomers (≈1:4 for complexes **6**, **8**, and **12**, and ≈2:3 for complex **10**), with the major rotamer being the one with its mesityl ring located above the benzylidene group.[21] The higher minor/major rotational isomer ratio in **10**, relative to that in complexes **6** and **8**, may be due to a more efficient slipped π–π stacking interaction between the 2,3,4,5,6-pentafluorophenyl and the benzylidene group in **10**, compared to the π–π interactions between the 2,6-difluorophenyl or the 2,4,6-trifluorophenyl and the benzylidene groups in **6** and **8**.[22] Single crystals of good quality for X-ray analysis from complexes **8**, **9**, and **13** were also obtained.[23] As depicted in Figures 1–3, all complexes exhibit a distorted square-pyramidal geometry with the Ru=C benzylidene bond occupying the apical position and the Cl atoms *trans* to one another. This geometry, as well as the bond lengths and angles in **8**, **9**, and **13**, are quite similar to those of parent complexes **3** and **5**. Moreover, in the solid state, the mesityl group in complexes **8**, **9**, and **11**[23] is located above the benzylidene moiety, as has been also observed in complexes **6** and **7**.[15]

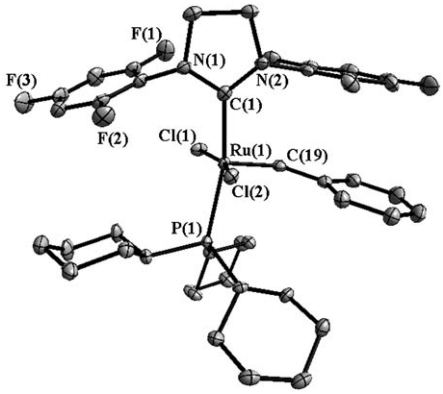

Figure 1. Crystal structure of catalyst **8**. Ellipsoids are drawn at 50% probability. Hydrogen atoms are omitted for clarity. Selected bond lengths [Å] and angles [°]: Ru(1)−C(19) 1.826(2), Ru(1)−C(1) 2.0602(18), Ru(1)−Cl(1) 2.3878(5), Ru(1)−Cl(2) 2.3927(4), Ru(1)−P(1) 2.4403(5), C(19)-Ru(1)-C(1) 97.61(8), C(19)-Ru(1)-Cl(1) 90.17(6), C(1)-Ru(1)-Cl(1) 93.25(5), C(19)-Ru(1)-Cl(2) 106.08(6), C(1)-Ru(1)-Cl(2) 83.33(5), Cl(1)-Ru(1)-Cl(2) 163.679(17), C(19)-Ru(1)-P(1) 96.29(6), C(1)-Ru(1)-P(1) 165.65(5), Cl(1)-Ru(1)-P(1) 90.246(16), Cl(2)-Ru(1)-P(1) 89.429(16).

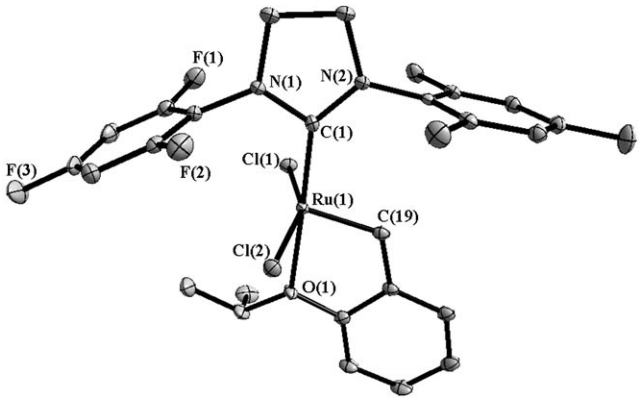

Figure 2. Crystal structure of catalyst **9**. Ellipsoids are drawn at 50% probability. Hydrogen atoms are omitted for clarity. Selected bond lengths [Å] and angles [°]: Ru(1)−C(19) 1.8307(18), Ru(1)−C(1) 1.9722(17), Ru(1)−O(1) 2.2502(12), Ru(1)−Cl(1) 2.3303(5), Ru(1)−Cl(2) 2.3420(5), C(19)-Ru(1)-C(1) 101.80(7), C(19)-Ru(1)-O(1) 79.79(6), C(1)-Ru(1)-O(1) 176.00(6), C(19)-Ru(1)-Cl(1) 103.00(6), C(1)-Ru(1)-Cl(1) 88.83(5), O(1)-Ru(1)-Cl(1) 87.23(4), C(19)-Ru(1)-Cl(2) 97.99(6), C(1)-Ru(1)-Cl(2) 97.05(5), O(1)-Ru(1)-Cl(2) 86.31(4), Cl(1)-Ru(1)-Cl(2) 156.547(17).

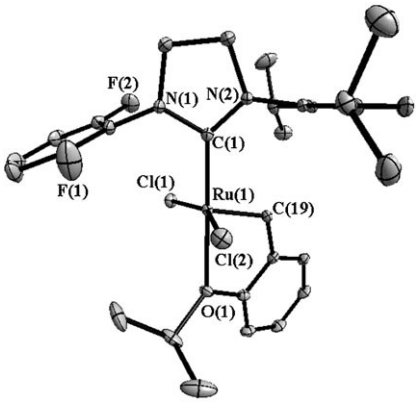

Figure 3. Crystal structure of catalyst **13**. Ellipsoids are drawn at 50% probability. Hydrogen atoms are omitted for clarity. Selected bond lengths [Å] and angles [°]: Ru(1)−C(22) 1.8340(9), Ru(1)−C(1) 1.9725(9), Ru(1)−O(1) 2.2451(7), Ru(1)−Cl(2) 2.3284(3), Ru(1)−Cl(1) 2.3393(2), C(22)-Ru(1)-C(1) 101.58(4), C(22)-Ru(1)-O(1) 79.87(3), C(1)-Ru(1)-O(1) 177.42(3), C(22)-Ru(1)-Cl(2) 104.07(3), C(1)-Ru(1)-Cl(2) 89.08(3), O(1)-Ru(1)-Cl(2) 88.49(2), C(22)-Ru(1)-Cl(1) 96.45(3), C(1)-Ru(1)-Cl(1) 96.34(3), O(1)-Ru(1)-Cl(1) 85.59(2), Cl(2)-Ru(1)-Cl(1) 157.287(9).

Ring-closing metathesis (RCM) activity of the new catalysts: RCM is the most frequently utilized olefin metathesis reaction in organic synthesis.[1b,24] We initially chose to study the catalytic activity of the new complexes in the RCM of di-

ethyldiallyl malonate (**19**) to disubstituted cycloalkene **20** by ^{1}H NMR spectroscopy (Figure 4). Interestingly, the plots of cycloalkene **20** conversion versus time reveal that both **6**

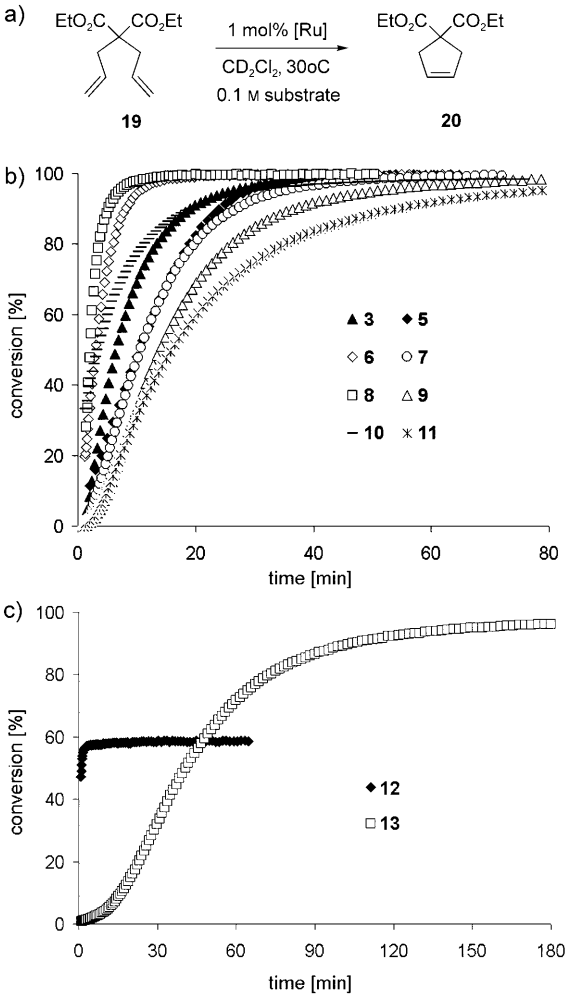

Figure 4. RCM of diene **19** with catalysts **3**, **5**, and **6–13**, at 30 °C.

and **8** effect the cyclization of **19** more efficiently than the second-generation phosphine-containing catalyst **3**, with catalyst **8** being the most efficient of all (>97% conversion in 9 min). Complex **10** is also more reactive than **3**, at least at the beginning of the RCM reaction (evidently due to its high initiation rate), but eventually slows down due to a decrease in its catalytic activity. This decrease in catalytic activity (decomposition) is also observed in the curvature in the ln[**19**] plot versus time for **10** (Supporting Information). Nevertheless, complex **10** eventually displays >97% conversion in 40 min. On the other hand, phosphine-free catalysts **7**, **9**, and **11** are less efficient than parent complex **3**. In fact, increasing the number of fluorine atoms on the *N*-aryl substituent, in going from complex **7** to **9** and eventually to **11**, results in lower activity, with catalyst **11** being the least efficient of all in this series (>97% conversion in 100 min). This low efficiency of catalyst **11** arises from its prolonged induction period and an increased decomposition rate, as illustrated from the curvature in the corresponding logarithmic plot (Supporting Information). Finally, as clearly illustrated in Figure 4, complexes **12** and **13** are very poor olefin metathesis catalysts. Phosphine-containing catalyst **12** exhibits high initial activity, but this activity decreases during the course of the reaction, due to its high decomposition rate, leveling off at 59% conversion. In sharp contrast, phosphine-free complex **13** has a very long induction period (11 min to reach 5% conversion), leading the reaction to >97% conversion in 180 min.

The RCM of diethylallylmethallyl malonate (**21**, Figure 5) leads to the formation of a trisubstituted five-membered

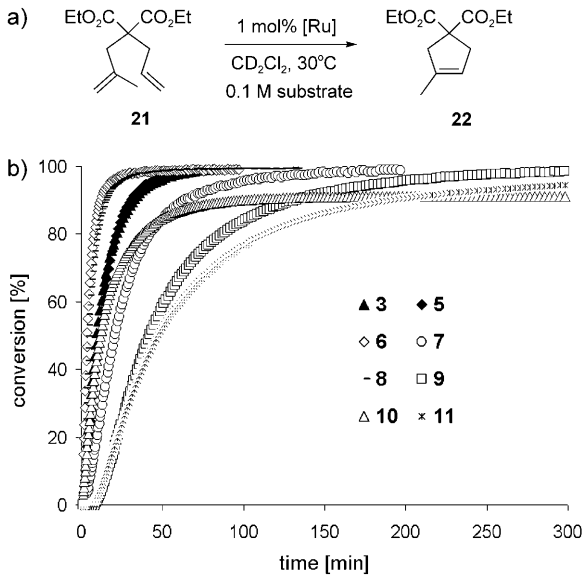

Figure 5. RCM of diene **21** with catalysts **3**, **5**, and **6–11**, at 30 °C.

ring (**22**). Due to steric effects, this reaction is more challenging than the RCM of diethyldiallyl malonate (**19**). Overall, the reactivity trends for this more demanding RCM reaction were found to be similar to those observed for the RCM of **19**. Thus, catalysts **6** and **8** show similar activity, being once again the most efficient catalysts in this study and outperforming second-generation catalysts **3** and **5**. Here, the reduced stability of catalyst **10** becomes more evident. After an initial period of high activity, the reaction rate slows drastically and eventually complex **10** does not catalyze this reaction to completion, reaching the final 90% conversion after 100 min. Complexes **12** and **13** are the most inefficient catalysts for this transformation in the present study. Under the standard reaction conditions (30 °C, 1% catalyst loading, 0.1 M substrate, CD_2Cl_2), **12** levels off at 30% conversion after 8 min, whereas it takes 13 h for complex **13** to lead the reaction to 95% conversion (Supporting Information).

The formation of tetrasubstituted double bonds through RCM is even more challenging and typically requires high catalyst loadings and elevated reaction temperatures due to

the increased steric bulk of the substrates.[9] In the model RCM reaction of diethyldimethallyl malonate catalysts **6** and **8** are the most efficient, affording 30% and 21% of the ring-closed product respectively, after four days at 30°C (Supporting Information). Complexes **11** and **13** do not ring-close diethyldimethallyl malonate. Catalysts **3** and **5** catalyze the same reaction in 17% and 6% respectively.

Ring-opening metathesis polymerization (ROMP) activity of the new catalysts: The ROMP of cyclic strained olefins is one of the earliest commercial application of olefin metathesis.[1,25] As such, we studied the catalytic activity of the new unsymmetrical catalysts in the ROMP of 1,5-cyclooctadiene (**23**) by ^{1}H NMR spectroscopy. The conversion to the product polyalkenamer (**24**) over time with catalysts **3** and **5–11** is represented in Figure 6. Interestingly, the reactivity trends

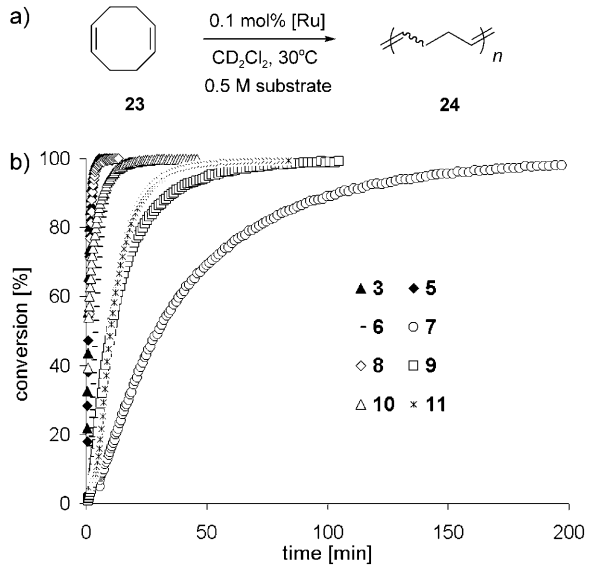

Figure 6. ROMP of **23** with catalysts **3**, **5**, and **6–11**, at 30°C.

observed for the fluorinated phosphine-free catalysts (**7**, **9**, and **11**) in RCM invert in the ROMP of 1,5-cyclooctadiene. Thus, catalyst **11** is the most reactive fluorinated phosphine-free catalyst, leading the reaction to >99% conversion in 60 min. In this reaction, complexes **3**, **5**, and **8** are the most efficient catalysts, showing very similar behavior with respect to reactivity. Moreover, since the stability of a catalyst does not have a very important impact in the ROMP of **23**,[24] complex **12** is also a competent catalyst in this reaction (>99% conversion in 13 min, Supporting Information).

Cross-metathesis (CM) activity of the new catalysts: When compared to RCM and ROMP, CM is certainly an underutilized olefin metathesis transformation. The basic reason lies in the fact that CM is more challenging, as it lacks the entropic driving force of RCM and the ring-strain release of ROMP. Additionally, CM reactions often lead to relatively low statistical yields of the desired cross-product, as well as poor *E*/*Z* cross-product selectivity.[26] It is also important to note that in CM, the *E*/*Z* selectivity at high conversion is governed by thermodynamic factors; that is, secondary metathesis promotes isomerization of the product to the thermodynamically favored *E* isomer. The development of catalysts that could efficiently control *E*/*Z* selectivity in CM reactions still represents a major challenge.[15,19,24,26] In our present study, we chose to evaluate catalysts **8–13** in the CM of allyl benzene (**25**) with *cis*-1,4-diacetoxy-2-butene (**26**). As shown in Figure 7, catalysts **6–11** demonstrate activity similar to or higher than the second-generation catalysts **3** and **5**. While catalysts **3** and **5** lead the reaction to 79% and 72% conversion, respectively, catalysts **9–11** are more efficient reaching a ≈88% yield of the desired cross-product (**27**). As illustrated in the plots of the *E*/*Z* ratio of cross-product versus conversion to cross-product (Figure 7), catalysts **6–11** are also more *Z* selective than catalysts **3** and **5**, at conversions above 60%. For example, catalyst **3** affords an *E*/*Z* ratio of ≈10 at 79% conversion, whereas at the same conversion catalysts **6–11** give an *E*/*Z* ratio of about 5.5.

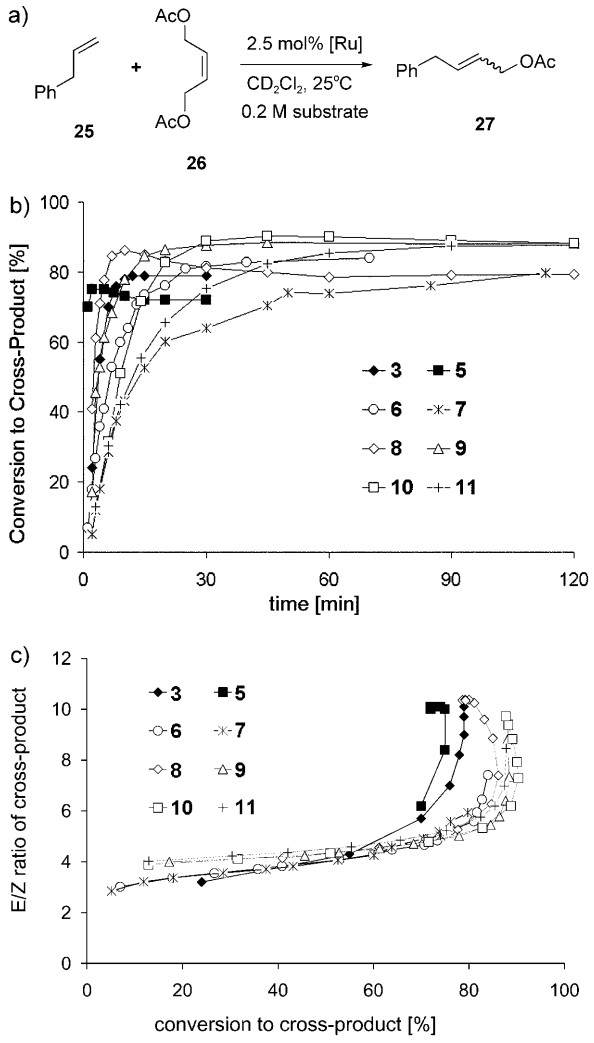

Figure 7. CM of **25** with **26** using catalysts **3**, **5**, and **6–11**.

Finally, complexes **12** and **13** are rather poor CM catalysts, showing lower reactivity than all other catalysts in this study. Additionally, the *E*/*Z* profile of catalysts **12** and **13** is very similar to that of catalysts **3** and **5** (Supporting Information).

Kinetic studies on the initiation of the new catalysts: We next determined the activation parameters for the initiation of catalysts **7**–**13** by utilizing the rapid, quantitative, and irreversible reaction of these complexes with butyl vinyl ether. This reaction affords a Fischer carbene, generally considered to be an inactive metathesis species.[27] The initiation experiments were carried out in [D_8]toluene (catalysts **8** and **10**–**13**) or [D_6]benzene (catalysts **7** and **9**), according to literature procedures.[28] The reactions between complexes **7**–**13** and butyl vinyl ether were carried out at four or five different temperatures, at 0.15 M olefin concentration; the activation parameters were then extracted from the resulting Eyring plots (Supporting Information). The obtained activation parameters are summarized in Table 1 and a representative Eyring plot is shown in Figure 8. To probe the dependence of the initiation rate on the olefin concentration, the initiation rates were also measured at 0.45 and 1.35 M olefin concentration at a selected temperature (Supporting Information).

Table 1. Activation parameters for the initiation of catalysts **3**, **5**, and **6**–**13**.

Catalyst	$\Delta H^{\neq}$ [kcal mol^{-1}]	$\Delta S^{\neq}$ [cal mol^{-1} K^{-1}]	$\Delta G^{\neq}$ (303 K) [kcal mol^{-1}]
3[a]	27±2	+13±6	23.0±0.4
6[b]	27±2	+19±9	21.78±0.08
8	26±2	+16±5	21.67±0.03
10	26±3	+15±9	22.05±0.07
5[c]	15.2±0.8	−19±3	20.69±0.02
7	12±2	−32±5	21.94±0.06
9	14±2	−26±7	22.09±0.08
11	16±1	−20±3	21.62±0.04
12	38±2	+66±8	17.9±0.2
13	17.6±0.7	−22±2	24.07±0.07

[a] Reference[28]. [b] Reference [15]. [c] Reference [29].

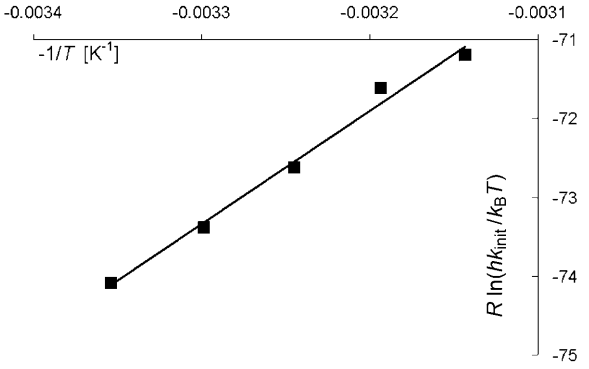

Figure 8. Eyring plot for the reaction of catalyst **9** with butyl vinyl ether.

The rate constants for all phosphine-containing catalysts were found to be independent of olefin concentration relative to [Ru], suggesting rate-determining phosphine dissociation. The large and positive values for $\Delta S^{\neq}$ for all phosphine-containing catalysts in Table 1 are also indicative of a dissociative mechanism.[28] Complex **12** has the lowest free energy of activation, being the fastest initiating catalyst in the present study. Unfortunately, as mentioned above, the lack of stability makes this complex a very poor olefin metathesis catalyst. As also illustrated in Table 1, catalysts **6** and **8** have essentially the same free energy of activation, initiating about 4 times faster than the parent complex **3**.

The rate constants in the reactions of the phosphine-free catalysts with butyl vinyl ether, in sharp contrast to the corresponding reactions of the phosphine-containing catalysts, show a first-order dependence on olefin concentration relative to [Ru] (Supporting Information). Moreover, the $\Delta S^{\neq}$ values for the phosphine-free complexes in Table 1 are both negative and large, also indicative of an associative mechanism. The values for $\Delta H^{\neq}$ in the two cases of phosphine-containing and phosphine-free catalysts are quite different as well.[30] Catalyst **13** has the highest free energy of activation in Table 1, being the poorest initiating catalyst in the present study. As discussed in the previous sections, this was also observed in the RCM, ROMP, and CM reactivity of catalyst **13**.

Studies on the electronic properties of the new unsymmetrical NHCs: Electron-rich and bulky NHC ligands display excellent σ-donating ability similar to electron-rich phosphines. One of the most straightforward methods to study the electronic properties of an NHC ligand is through the measurement of the carbonyl stretching frequencies in the corresponding [$Rh(CO)_2X(NHC)$] complexes.[31] Since the CO stretching frequencies (wavenumbers) in these complexes are inversely proportional to the π-back-donation from the metal center, the more basic the NHC the more important the π-back-donation from the metal and, therefore, the lower the stretching frequency of the CO ligands. Chlorodicarbonyl(carbene)rhodium(I) complexes **29**–**33** were easily prepared by transmetalation from the corresponding Ag^I complexes. For the preparation of **29**, **30**, and **32** we used [{$Rh(CO)_2Cl$}$_2$] as rhodium source, whereas in the case of **31** and **33** we used [{Rh(cod)Cl}$_2$] (cod = cyclooctadiene). Complex **32**, bearing a symmetrical NHC with *o*-fluorinated aryl groups, was synthesized for comparison reasons.[32] FT-IR spectroscopy of complexes **29**–**33** was carried out in CH_2Cl_2. The measured CO stretching frequencies I and II (Table 2) indicate that the parent ligand (H_2IMes) has the highest σ-donating ability in this series of ligands. In contrast, the ligand that induces the lowest electron density at the metal center is the tetrafluorinated symmetrical NHC in **32**, with the unsymmetrical *N*-pentafluorophenyl NHC in **31** being the second least basic ligand. Finally, the NHCs in Rh complexes **29**, **30**, and **33** have identical σ-donor and π-acceptor properties. Overall, there is a shift of the CO stretching frequencies in Rh complexes **28**–**33** as a function

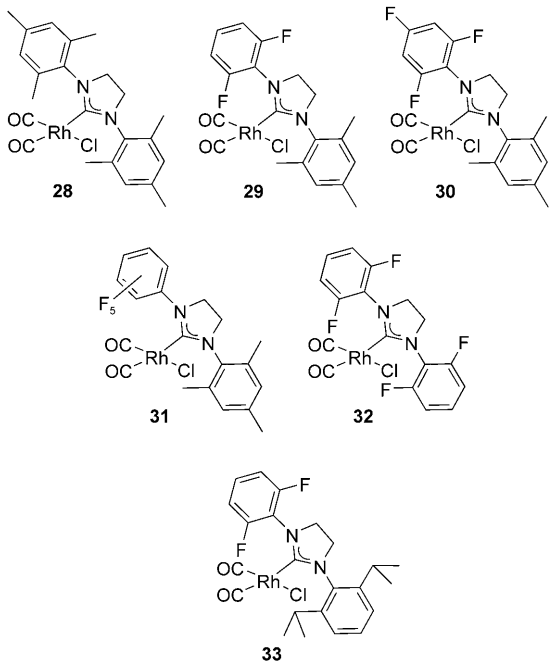

Table 2. Carbonyl stretching frequencies for rhodium complexes **28–33**.

Compound	$\nu_{CO\,I}$ [cm^{-1}]	$\nu_{CO\,II}$ [cm^{-1}]
28[a]	2081	1996
29	2081	2000
30	2081	2000
31	2083	2005
32	2085	2005
33	2081	2000

[a] Reference [31a].

of the number of fluorine atoms on the *N*-aryl sybstituents of the NHC. However, with the exception of the phosphine-free catalysts in RCM reactions, there is no evident correlation between the electronic properties of the NHCs and the efficiency of the corresponding ruthenium catalysts for the present series of catalysts.[33]

Conclusion

A series of ruthenium-based metathesis catalysts bearing unsymmetrical NHC ligands has been prepared and completely characterized. All of these complexes are competent catalysts for ring-closing metathesis, cross metathesis, and ring-opening metathesis polymerization, in some cases surpassing in efficiency the existing second-generation catalysts. In the cross metathesis of allyl benzene with *cis*-1,4-diacetoxy-2-butene, all new catalysts afford improved *E*/*Z* ratios of the desired cross-product at conversions above 60%. The influence of the unsymmetrical NHC ligands on the initiation rate and the activation parameters in the reaction of the corresponding ruthenium complexes with butyl vinyl ether was also studied. The results from these experiments suggest initiation of the phosphine-containing catalysts by the well-established dissociative mechanism. In the case of the phosphine-free catalysts the initiation mechanism is most probably associative. Finally, the synthesis of the related $[Rh(CO)_2Cl(NHC)]$ complexes allowed the study of the electronic properties of the new unsymmetrical NHC ligands. It was found that although there is a shift of the CO stretching frequencies in these Rh complexes as a function of the number of fluorine atoms on the *N*-aryl substituents of the NHC, there is no correlation between the electronic properties of the NHCs and the efficiency of the corresponding ruthenium catalysts for the present series of catalysts.

Experimental Section

Materials and general procedures: Unless otherwise indicated, all compounds were purchased from Aldrich or Fisher. Catalyst **2** was obtained from Materia. Silica gel used for the purification of organometallic complexes was obtained from TSI Scientific, Cambridge, MA (60 Å, pH 6.5–7.0). Oxomesitylacetyl chloride was prepared by a method reported by Mol and co-workers.[11] All reactions involving metal complexes were conducted in oven-dried glassware under an argon or nitrogen atmosphere with anhydrous solvents, by using standard Schlenk and glovebox techniques. Anhydrous solvents were obtained by elution through a solvent column drying system.[34] The screening of the catalysts, in ring-closing metathesis, cross metathesis, and ring-opening metathesis polymerization reactions was conducted according to literature procedures.[24] NMR spectra were measured on Varian Inova 500 and Varian Mercury 300 spectrometers. NMR chemical shifts are reported in ppm downfield from Me_4Si, by using the residual solvent peak as internal standard for ^1H and ^{13}C, and H_3PO_4 ($\delta = 0.0$ ppm) for ^{31}P. Gas chromatography data was obtained using an Agilent 6850 FID gas chromatograph equipped with a DB-Wax Polyethylene Glycol capillary column (J&W Scientific). IR spectra were recorded on a Perkin-Elmer Paragon 1000 spectrophotometer. X-ray crystallographic structures were obtained by Larry M. Henling and Dr. Michael W. Day of the California Institute of Technology Beckman Institute X-ray Crystallography Laboratory. CCDC-660407 (**8**), CCDC-660408 (**9**) and CCDC-627196 (**13**) contain the supplementary crystallographic data for this paper. These data can be obtained free of charge from The Cambridge Crystallographic Data Centre via www.ccdc.cam.ac.uk/data_request/cif.

***N*-(2,4,6-Trifluorophenyl)oxanilic acid ethyl ester (15a)**: 2,4,6-Trifluoroaniline (2.94 g, 20.0 mmol, 1.0 equiv) and dry triethylamine (2.79 mL, 20.0 mmol, 1.0 equiv) were dissolved in dry THF (40 mL) under nitrogen. This solution was cooled to 0°C, and ethyl chlorooxoacetate (2.22 mL, 20.0 mmol, 1.0 equiv) was added dropwise. Precipitation of a white solid (triethylammonium chloride) occurred immediately upon addition. The suspension was allowed to stir for 16 h, warming to room temperature. The solid was filtered off, washed with diethyl ether (50 mL), and the combined organic layer was washed with an aqueous saturated NH_4Cl solution until pH 6. This organic layer was then washed with brine (80 mL) and dried over $MgSO_4$. The solvent was removed under reduced pressure, leaving a yellow solid that was washed with hexanes (3×6 mL) to afford **15a** as a white crystalline solid (3.31 g, 13.4 mmol, 67% yield). ^1H NMR (300 MHz, $CDCl_3$, 25°C): $\delta = 8.31$ (br s, 1H), 6.81–6.76 (m, 2H), 4.43 (q, $^3J(H,H) = 7$ Hz, 2H), 1.44 ppm (t, $^3J(H,H) = 7$ Hz, 3H); $^{13}C\{^1H\}$ NMR (75 MHz, $CDCl_3$, 25°C; due to extensive fluorine coupling, coupling constants are not given and resonances are reported as peaks): $\delta = 163.47$–163.08 (m), 160.02–159.69 (m), 156.62–156.32 (m), 154.90, 101.50–100.78 (m), 64.11, 14.16 ppm; $^{19}F\{^1H\}$ NMR (282 MHz, $CDCl_3$, 25°C): $\delta = -107.80$, -113.93 ppm; HRMS (FAB$^+$): m/z calcd for $C_{10}H_9NO_3F_3$ [M^+]: 248.0535; found: 248.0536.

***N*-(2,4,6-Trifluorophenyl)-*N'*-mesityloxalamide (16a)**: Compound **15a** (2.47 g, 10.0 mmol, 1.0 equiv) was suspended in 2,4,6-trimethylaniline (2.53 mL, 18.0 mmol, 1.8 equiv) in a dry Schlenk tube under nitrogen. The tube was sealed and the suspension was stirred at 180 °C for 16 h. Upon being cooled to room temperature, the reaction mixture solidified. The orange-brown solid was washed with diethyl ether (4×5 mL) and hexanes (2×5 mL), leaving **16a** as a white solid (1.41 g, 4.2 mmol, 42 % yield). ^{1}H NMR (300 MHz, $CDCl_3$, 25 °C): δ = 9.07 (brs, 1H), 8.81 (brs, 1H), 6.90 (s, 2H), 6.79–6.74 (m, 2H), 2.29 (s, 3H), 2.18 ppm (s, 6H); ^{13}C{^{1}H} NMR (75 MHz, $CDCl_3$, 25 °C; due to extensive fluorine coupling, coupling constants are not given and resonances are reported as peaks): δ = 159.91–159.62 (m), 158.74, 157.41, 156.55–156.25 (m), 137.94, 134.93, 129.58, 129.26, 101.44–100.71 (m), 21.17, 18.52 ppm; ^{19}F{^{1}H} NMR (282 MHz, $CDCl_3$, 25 °C): δ = −108.18, −113.65 ppm; HRMS (FAB$^+$): *m*/*z* calcd for $C_{17}H_{16}N_2O_2F_3$ [M^+]: 337.1164; found: 337.1164.

***N*-(2,4,6-Trifluorophenyl)-*N'*-mesityl-1,2-ethanediamine dihydrochloride (17a)**: In a dry, high pressure tube containing **16a** (1.68 g, 5.0 mmol, 1.0 equiv), BH_3·THF (1 M in THF) (25 mL, 25.0 mmol, 5.0 equiv) was added under nitrogen. The tube was sealed and the solution was stirred at 70 °C for 16 h. Once the reaction mixture had cooled to room temperature, the clear yellowish solution was slowly added to methanol (50 mL) at 0 °C. Concentrated aqueous HCl solution (1.8 mL) was also slowly added at 0 °C. When all bubbling ceased, the solvent was removed under reduced pressure. The resulting solid was dissolved in methanol and the solvent was again removed under reduced pressure. This was repeated twice more to remove the remaining boron as $B(OMe)_3$. The remaining white solid was finally washed with diethyl ether (2×5 mL) to provide the desired product as a white powder (1.53 g , 4.0 mmol, 80 % yield). ^{1}H NMR (300 MHz, [D$_6$]DMSO, 25 °C): δ = 7.11–7.05 (m, 2H), 6.96 (s, 2H), 3.59–3.33 (m, 4H), 2.48 (s, 6H), 2.37 ppm (s, 3H); ^{13}C{^{1}H} NMR (75 MHz, [D$_6$]DMSO, 25 °C; due to extensive fluorine coupling, coupling constants are not given and resonances are reported as peaks): δ = 152.51–152.34 (m), 138.26, 131.82, 130.31, 124.95–124.60 (m), 116.97–116.64 (m), 111.86–111.43 (m), 50.57, 41.32, 20.16, 17.57 ppm; ^{19}F{^{1}H} NMR (300 MHz, [D$_6$]DMSO, 25 °C): δ = −123.19, −125.29 ppm; HRMS (FAB$^+$): *m*/*z* calcd for $C_{17}H_{20}N_2F_3$ [M^+]: 309.1579; found: 309.1587.

1-(2,4,6-Trifluorophenyl)-3-mesityl-4,5-dihydroimidazolium chloride (18a): A suspension of **17a** (1.53 g, 4.0 mmol, 1.0 equiv) in triethylorthoformate (13.3 mL, 80.0 mmol, 20.0 equiv) was heated at 135 °C for 30 min under nitrogen. Upon cooling to room temperature, the solids were filtered of and washed with diethyl ether (3×10 mL) to provide the desired product as a white solid (1.28 g , 3.6 mmol, 90 % yield). ^{1}H NMR (300 MHz, [D$_6$]DMSO, 25 °C): δ = 9.59 (s, 1H), 7.64–7.58 (m, 2H), 7.07 (s, 2H), 4.58–4.64 (m, 4H), 2.30 (s, 6H), 2.26 ppm (s, 3H); ^{13}C{^{1}H} NMR (75 MHz, [D$_6$]DMSO, 25 °C; due to extensive fluorine coupling, coupling constants are not given and resonances are reported as peaks): δ = 162.15–161.19 (m), 140.54, 135.78, 131.32, 130.17, 124.97–124.79 (m), 111.93–111.39 (m), 103.15–102.37 (m), 52.20, 52.06, 21.24, 17.78 ppm; ^{19}F{^{1}H} NMR (282 MHz, [D$_6$]DMSO, 25 °C): δ = −105.45, −116.29 ppm; HRMS (FAB$^+$): *m*/*z* calcd for $C_{18}H_{18}N_2F_3$ [M^+]: 319.1422; found: 319.1421.

[RuCl$_2${1-(2,4,6-trifluorophenyl)-3-mesityl-4,5-dihydroimidazol-2-ylidene}-(=CH−Ph)(PCy$_3$)] (8): In a glove box, **18a** (355 mg, 1.0 mmol, 2.0 equiv) and KHMDS (337 mg, 1.0 mmol, 2.0 equiv) were stirred in benzene (10 mL) at room temperature for 30 min. Catalyst **2** (411 mg, 500 μmol, 1.0 equiv) was added as a solid in one portion, and the reaction flask was taken out of the glove box and heated under a nitrogen atmosphere at 80 °C for 30 min. The solution was concentrated to 2 mL in vacuo and poured onto a column packed with TSI Scientific silica gel. The complex was eluted with hexanes/diethyl ether (2:1) as a red band. This was concentrated in vacuo, transferred in a glove box, dissolved in the minimum amount of benzene and lyophilized to afford the desired complex as a violet solid (345 mg, 401 μmol, 80 % yield). Crystals suitable for X-ray crystallography were grown at room temperature by slow diffusion of hexanes into a solution of **8** in benzene. ^{1}H NMR (500 MHz, CD_2Cl_2, 25 °C): δ = 19.48 (s, 1H-minor), 19.12 (s, 1H-major), 7.47–6.88 (m, 9H-major, 9H-minor), 4.10–3.90 (m, 4H-major, 4H-minor), 2.62–1.00 ppm (m, 42H-major, 42H-minor); ^{13}C{^{1}H} NMR (125 MHz, CD_2Cl_2, 25 °C; due to extensive fluorine coupling and the existence of two rotational isomers, coupling constants are not given and resonances are reported as peaks): δ = 297.57 (major), 293.43 (minor), 223.44, 222.80, 164.00–163.84 (m), 162.94–162.76 (m), 160.89–160.69 (m), 155.69–155.42 (m), 152.31–152.21 (m), 152.02–151.86 (m), 151.21, 142.89–142.75 (m), 138.87, 138.24, 136.90–136.77 (m), 136.59, 135.09, 131.02–130.50 (m), 130.00, 129.18, 128.91, 128.53, 128.02–127.83 (m), 101.87–101.44 (m), 101.03–100.60 (m), 53.10–53.05 (m), 52.76, 52.22, 52.20, 32.15, 32.02, 31.96, 31.83, 29.26, 28.00, 27.92, 27.84, 26.39, 26.36, 21.07, 20.86, 19.68, 18.28 ppm; ^{31}P{^{1}H} NMR (121 MHz, CD_2Cl_2, 25 °C) δ = 31.94 (s, minor), 27.33 ppm (s, major); ^{19}F{^{1}H} NMR (282 MHz, CD_2Cl_2, 25 °C): δ = −105.01 (d, major, J_{FF} = 18 Hz), −106.15 (brs, major), −108.25 (d, minor, J_{FF} = 18 Hz), −114.02 ppm (brs, minor); HRMS (FAB$^+$): *m*/*z* calcd for $C_{43}H_{56}N_2F_3Cl_2PRu$ [M^+]: 860.2554; found: 860.2536.

[RuCl$_2$(1-(2,4,6-trifluorophenyl)-3-mesityl-4,5-dihydroimidazol-2-ylidene)(=CH-*o*-*i*PrO−Ph)] (9): In a glovebox, a vial was charged with complex **8** (172 mg, 200 μmol, 1.0 equiv), toluene (4 mL), and *o*-isopropoxy-β-methylstyrene (175 mg, 4.0 mmol, 20.0 equiv). The dark red solution was stirred for 10 min and then left inside the capped vial without stirring at room temperature. After 48 h the desired complex had precipitated as dark green crystals. The supernatant brown liquid was decanted off; the crystals were washed with pentanes (3×10 mL) and dried in vacuo to afford complex **9** (109 mg, 171 μmol, 85 % yield). Crystals suitable for X-ray crystallography were grown at room temperature by slow diffusion of hexanes into a solution of **9** in benzene. ^{1}H NMR (500 MHz, CD_2Cl_2, 25 °C): δ = 16.10 (s, 1H), 7.56–7.53 (m, 2H), 7.12 (s, 2H), 6.94–6.89 (m, 4H), 5.00 (septet, ^3J(H,H) = 6 Hz, 1H), 4.25–4.15 (m, 4H), 2.47 (s, 3H), 2.30 (s, 6H), 1.36 ppm (d, ^3J(H,H) = 6 Hz, 6H); ^{13}C{^{1}H} NMR (125 MHz, CD_2Cl_2, 25 °C; due to extensive fluorine coupling, coupling constants are not given and resonances are reported as peaks): δ = 292.19, 215.59, 164.56–164.32 (m), 163.31–163.14 (m), 163.31–163.14 (m), 162.43–162.32 (m), 161.27–161.10 (m), 152.45, 144.53, 139.46, 137.93, 137.50, 129.91, 129.85, 122.61, 122.51, 113.11, 101.45–101.04 (m), 75.50, 53.15, 51.84, 21.29, 21.16, 17.96 ppm; ^{19}F{^{1}H} NMR (282 MHz, CD_2Cl_2, 25 °C): δ = −103.97, −106.17 ppm; HRMS (FAB$^+$): *m*/*z* calcd for $C_{28}H_{29}N_2OF_3Cl_2Ru$ [M^+]: 638.0653; found: 638.0658.

***N*-(2,3,4,5,6-Pentafluorophenyl)-*N'*-mesityloxalamide (16b)**: Compound **15b** (1.35 g, 6.0 mmol, 1.0 equiv) was added to a solution of 2,3,4,5,6-pentafluoroaniline (2.42 g, 13.2 mmol, 2.2 equiv) in dry THF (60 mL) under nitrogen. After stirring the reaction mixture at room temperature for 2 h, the solvent was evaporated under reduced pressure. The remaining solid was washed with hexanes (3×10 mL) and dried under high vacuum to afford the desired compound as a white solid (2.12 g, 5.7 mmol, 95 % yield). ^{1}H NMR (300 MHz, $CDCl_3$, 25 °C): δ = 9.14 (brs, 1H), 8.68 (brs, 1H), 6.92 (s, 2H), 2.30 (s, 3H), 2.20 ppm (s, 6H); ^{13}C{^{1}H} NMR (75 MHz, $CDCl_3$, 25 °C; due to extensive fluorine coupling, coupling constants are not given and resonances are reported as peaks): δ = 158.68, 157.12, 144.83–144.44 (m), 142.61–142.14 (m), 141.48–141.19 (m), 139.85–139.41 (m), 139.23–138.75 (m), 138.10, 136.55–136.06 (m), 134.80, 129.30, 129.12, 111.07–110.52 (m), 21,08, 18.34 ppm; ^{19}F{^{1}H} NMR (282 MHz, $CDCl_3$, 25 °C): δ = −143.95 (d, J(^{19}F,^{19}F) = 18 Hz), −155.28 to −155.45 (m), −161.85 ppm (t, J(^{19}F,^{19}F) = 18 Hz); HRMS (EI$^+$): *m*/*z* calcd for $C_{17}H_{13}N_2O_2F_5$ [M^+]: 372.0897; found: 372.0893.

***N*-(2,3,4,5,6-Pentafluorophenyl)-*N'*-mesityl-1,2-ethanediamine dihydrochloride (17b)**: This was synthesized analogously to **17a** starting with **16b** (white powder, 60 % isolated yield). ^{1}H NMR (300 MHz, [D$_6$]DMSO, 25 °C): δ = 6.95 (s, 2H), 3.76 (t, ^3J(H,H) = 6 Hz, 2H), 3.39 (t, ^3J(H,H) = 6 Hz, 2H), 2.44 (s, 6H), 2.20 ppm (s, 3H); ^{13}C{^{1}H} NMR (75 MHz, [D$_6$]DMSO, 25 °C; due to extensive fluorine coupling, coupling constants are not given and resonances are reported as peaks): δ = 139.92–139.63 (m), 139.50–139.18 (m), 138.99, 136.89–136.01 (m), 134.25–133.88 (m), 132.60, 131.39, 130.99, 124.46–124.12 (m), 50.94, 41.81, 20.81, 18.39 ppm; ^{19}F{^{1}H} NMR (282 MHz, [D$_6$]DMSO, 25 °C): δ = −159.54 to −159.65 (m), −165.66 to −165.81 (m), −174.82 to −174.92 ppm (m); HRMS (FAB$^+$): *m*/*z* calcd for $C_{17}H_{18}N_2F_5$ [M^+]: 345.1390; found: 345.1396.

1-(2,3,4,5,6-Pentafluorophenyl)-3-mesityl-4,5-dihydroimidazolium chloride (18b): A suspension of **17b** (834 mg, 2.0 mmol, 1.0 equiv) in triethylorthoformate (6.6 mL, 40.0 mmol, 20.0 equiv) was heated at 135 °C for

5 min under argon. After cooling to room temperature, the solids were filtered of and washed with diethyl ether (4×2 mL) to provide the desired product as a white solid (622 mg, 1.7 mmol, 87% yield). ^{1}H NMR (300 MHz, $CDCl_3$, 25°C): δ=10.47 (s, 1H), 6.89 (s, 2H), 4.68 (t, ^3J(H,H)=11 Hz, 2H), 4.46 (t, ^3J(H,H)=11 Hz, 2H), 2.26 ppm (s, 9H); ^{13}C{^{1}H} NMR (75 MHz, $CDCl_3$, 25°C; due to extensive fluorine coupling, coupling constants are not given and resonances are reported as peaks): δ=162.10, 145.21–144.94 (m), 143.99–143.48 (m), 141.87–141.69 (m), 141.16, 139.96–139.65 (m), 136.66–136.27 (m), 134.78, 130.25, 130.08, 111.98–111.54 (m), 52.59, 52.03, 21.25, 17.92 ppm; ^{19}F{^{1}H} NMR (282 MHz, $CDCl_3$, 25°C): δ=−145.77 to −145.84 (m), −151.62 to −151.75 (m), −160.23 to −160.36 ppm (m); HRMS (FAB$^+$) *m/z* calcd for $C_{18}H_{16}N_2F_5$ [M^+]: 355.1234; found: 355.1245.

[RuCl$_2${1-(2,3,4,5,6-pentafluorophenyl)-3-mesityl-4,5-dihydroimidazol-2-ylidene}(=CH−Ph)(PCy$_3$)] (10): In a glove box, **18b** (195 mg, 500 μmol, 2.0 equiv), KHMDS (100 mg, 500 μmol, 2.0 equiv), and complex **2** (206 mg, 250 μmol, 1.0 equiv) were simultaneously dissolved in benzene (5 mL). The reaction flask was taken out of the glove box and heated under a nitrogen atmosphere at 80°C for 20 min. The solution was concentrated to 2 mL in vacuo and poured onto a column packed with TSI Scientific silica gel. The complex was eluted with hexanes/diethyl ether (2:1) as a red band. This was concentrated in vacuo, transferred in a glove box, dissolved in the minimum amount of benzene and lyophilized to afford the desired complex as a violet solid (170 mg, 190 μmol, 76% yield). ^{1}H NMR (300 MHz, CD_2Cl_2, 25°C): δ=19.66 (s, 1H-minor), 19.07 (s, 1H-major), 7.55–6.99 (m, 7H-major, 7H-minor), 4.16–3.81 (m, 4H-major, 4H-minor), 2.64–1.01 ppm (m, 42H-major, 42H-minor); ^{13}C{^{1}H} NMR (125 MHz, CD_2Cl_2, 25°C; due to extensive fluorine coupling and the existence of two rotational isomers, coupling constants are not given and resonances are reported as peaks): δ=297.98 (major), 292.73 (minor), 223.71 (d, ^2J(^{13}C,^{31}P)=18 Hz), 223.10 (d, ^2J(^{13}C,^{31}P)=13 Hz), 164.82, 151.35, 150.71, 147.48–147.31 (m), 146.29–145.92 (m), 145.53–145.28 (m), 144.20–143.92 (m), 143.25–143.00 (m), 139.05–138.66 (m), 138.24–138.00 (m), 137.23–136.85 (m), 136.48–136.25 (m), 135.93, 134.34, 131.60–131.22 (m), 130.67–130.20 (m), 129.75, 129.54, 128.993, 128.51, 127.83–127.44 (m), 126.41–126.14 (m), 125.41–125.10 (m), 117.56–117.31 (m), 116.00–115.76 (m), 52.63, 52.49, 52.16, 31.87, 31.74, 31.69, 31.56, 29.00, 27.63, 27.55, 27.51, 27.43, 26.08, 25.98, 20.74, 20.54, 19.31, 17.92 ppm; ^{31}P{^{1}H} NMR (121 MHz, CD_2Cl_2, 25°C) δ=32.47 (s, minor), 27.04 ppm (s, major); ^{19}F{^{1}H} NMR (282 MHz, CD_2Cl_2, 25°C): δ=−136.09, −144.05, −144.35, −152.96 (t, J(^{19}F,^{19}F)=24 Hz), −155.60 (t, J(^{19}F,^{19}F)=24 Hz), −161.35, −161.42, −161.79 (brs), −162.39 (brs), −163.45 (brs), −166.07 ppm (t, J(^{19}F,^{19}F)=24 Hz); HRMS (FAB$^+$): *m/z* calcd for $C_{43}H_{54}N_2F_5Cl_2PRu$ [M^+]: 896.2366; found: 896.2363.

[RuCl$_2${1-(2,3,4,5,6-pentafluorophenyl)-3-mesityl-4,5-dihydroimidazol-2-ylidene}(=CH-*o*-*i*PrO−Ph)] (11): Inside a glovebox, a vial was charged with complex **10** (120 mg, 134 μmol, 1.0 equiv), toluene (2 mL), and *o*-isopropoxy-β-methylstyrene (472 mg, 2.7 mmol, 20.0 equiv). The deep red solution was stirred for 20 min and then left inside the capped vial without stirring at room temperature. After 48 h the vial was removed from the glove box and placed in an oil bath at 60°C for 30 min. Upon cooled to room temperature, the reaction mixture was poured onto a column packed with TSI Scientific silica gel. The complex was eluted with hexanes/diethyl ether (2:1) as a green band. This was concentrated in vacuo, transferred in a glove box, dissolved in the minimum amount of benzene and lyophilized. The obtained solid was finally washed with pentanes (4×1 mL) to afford the desired complex as a green powder (52 mg, 77 μmol, 57% yield). Crystals suitable for X-ray crystallography were grown at room temperature by slow diffusion of hexanes into a solution of **11** in benzene. ^{1}H NMR (300 MHz, CD_2Cl_2, 25°C): δ=16.00 (s, 1H), 7.58–7.53 (m, 1H), 7.12 (s, 2H), 6.97–6.90 (m, 3H), 5.04 (septet, ^3J(H,H)=6 Hz, 1H), 4.28–4.19 (m, 4H), 2.46 (s, 3H), 2.29 (s, 6H), 1.40 ppm (d, ^3J(H,H)=6 Hz, 6H); ^{13}C{^{1}H} NMR (125 MHz, CD_2Cl_2, 25°C; due to extensive fluorine coupling, coupling constants are not given and resonances are reported as peaks): δ=271.96, 216.34, 152.21, 147.67–147.59 (m), 145.62–145.57 (m), 143.97, 143.42–143.16 (m), 141.37–141.11 (m), 139.36, 139.21–138.84 (m), 137.41, 136.86, 129.92, 129.60, 122.34, 115.85–115.59 (m), 112.84, 75.27, 51.58, 20.95, 20.83, 17.61 ppm; ^{19}F{^{1}H} NMR (282 MHz, CD_2Cl_2, 25°C): δ=−134.98 (d, J(^{19}F,^{19}F)=18 Hz), −154.02 (t, J(^{19}F,^{19}F)=24 Hz), −163.46 ppm (t, J(^{19}F,^{19}F)=24 Hz); HRMS (FAB$^+$): *m/z* calcd for $C_{28}H_{27}N_2F_5Cl_2ORu$ [M^+]: 674.0465; found: 674.0437.

Phenyl chlorooxoacetate (14c): Phenol (15.64 g, 166.2 mmol, 1.0 equiv) was dissolved in dry CH_2Cl_2 (150 mL) and oxalyl chloride (14.5 mL, 166.2 mmol, 1.0 equiv) was slowly added through a syringe. This solution was cooled to 0°C and dry triethylamine (23.2 mL, 166.2 mmol, 1.0 equiv) was added dropwise over a period of 30 min. Precipitation of a white solid (triethylammonium chloride) was observed. The final orange suspension was allowed to stir for 45 min as the reaction mixture warmed to room temperature. The solid was filtered off, and the solvent of the filtrate was removed under reduced pressure to afford a tan solid. This was suspended in hexanes (200 mL) and filtrated again to remove the remaining triethylammonium chloride. The solvent was removed under reduced pressure to afford **14c** as an off-white solid (16.95 g, 92.1 mmol, 55% yield). ^{1}H NMR (300 MHz, $CDCl_3$, 25°C): δ=7.55–7.50 (m, 2H), 7.44–7.40 (m, 1H), 7.34–7.32 ppm (m, 2H); ^{13}C{^{1}H} NMR (75 MHz, $CDCl_3$, 25°C): δ=161.38, 154.26, 150.39, 130.27, 127.66, 120.94 ppm; HRMS (EI$^+$): *m/z* calcd for $C_8H_5ClO_3$ [M^+]: 183.9927; found: 183.9928.

***N*-(2,6-Difluorophenyl)oxanilic acid phenyl ester (15c)**: 2,6-difluoroaniline (5.05 mL, 50.0 mmol, 1.0 equiv) and dry triethylamine (13.9 mL, 100.0 mmol, 2.0 equiv) were dissolved in dry THF (250 mL) under nitrogen. This solution was cooled to 0°C, and **14c** (11.07 g, 60.0 mmol, 1.2 equiv) was added in one portion. Precipitation of a white solid (triethylammonium chloride) occurred immediately upon addition. The suspension was allowed to stir for 16 h as the reaction mixture warmed to room temperature. The solid was filtered off and washed with diethyl ether (200 mL). The combined organic layer was initially washed with an aqueous saturated NH_4Cl solution, until pH 6, then with brine (300 mL), and dried over Na_2SO_4. The solvent was removed under reduced pressure leaving a red viscous liquid that was vigorously stirred with hexanes until a white-pink solid precipitated. This was washed with hexanes (3×6 mL) to afford **15c** as a white solid (9.32 g, 33.6 mmol, 67% yield). ^{1}H NMR (300 MHz, $CDCl_3$, 25°C): δ=8.48 (brs, 1H), 7.48–7.41 (m, 2H), 7.35–7.17 (m, 4H), 7.04 ppm (t, ^3J(H,H)=8 Hz, 2H); ^{13}C{^{1}H} NMR (75 MHz, $CDCl_3$, 25°C; due to extensive fluorine coupling, coupling constants are not given and resonances are reported as peaks): δ=159.51, 159.45, 158.79, 156.16, 156.10, 154.45, 150.40, 146.84, 129.93, 129.23, 129.10, 128.98, 127.09, 121.19, 112.41–112.29 (m), 112.14–112.06 ppm (m); ^{19}F{^{1}H} NMR (282 MHz, $CDCl_3$, 25°C): δ=−117.01; HRMS (FAB$^+$): *m/z* calcd for $C_{14}H_{10}NO_3F_2$ [M^+]: 278.0629; found: 278.0637.

***N*-(2,6-Difluorophenyl)-*N*′-(2,6-diisopropylphenyl)oxalamide (16c)**: Compound **15c** (5.54 g, 20.0 mmol, 1.0 equiv) was suspended in 2,6-diisopropylaniline (12.68 mL, 70.0 mmol, 3.5 equiv) in a dry Schlenk tube under nitrogen. The tube was sealed and the suspension was stirred at 180°C for 16 h. The resulting brown solid was washed with hexanes (5×15 mL) leaving **16c** as a white solid (5.05 g, 14.0 mmol, 70% yield). ^{1}H NMR (300 MHz, $CDCl_3$, 25°C): δ=8.94 (brs, 1H), 8.75 (brs, 1H), 7.39–7.22 (m, 4H), 7.04 (t, ^3J(H,H)=8 Hz, 2H), 3.05 ppm (septet, ^3J(H,H)=7 Hz, 2H), 1.22 (d, ^3J(H,H)=7 Hz, 12H); ^{13}C{^{1}H} NMR (75 MHz, $CDCl_3$, 25°C; due to extensive fluorine coupling, coupling constants are not given and resonances are reported as peaks): δ=158.56, 158.41, 156.02, 155.81, 153.22, 146.06, 129.50, 129.25, 128.72, 123.99, 112.41–112.33 (m), 112.18–112.10 (m), 29.16, 23.89 ppm; ^{19}F{^{1}H} NMR (282 MHz, $CDCl_3$, 25°C): δ=−116.95 ppm; HRMS (FAB$^+$): *m/z* calcd for $C_{20}H_{23}N_2O_2F_2$ [M^+]: 361.1728; found: 361.1731.

***N*-(2,6-Difluorophenyl)-*N*′-(2,6-diisopropylphenyl)-1,2-ethanediamine dihydrochloride (17c)**: This compound was synthesized analogously to **17a** starting with **16c** (white powder, 67% isolated yield). ^{1}H NMR (300 MHz, [D$_6$]DMSO, 25°C): δ=7.41–7.20 (m, 3H), 6.99–6.94 (m, 2H), 6.73–6.63 (m, 1H), 3.76–3.66 (m, 2H), 3.28–3.19 (m, 4H), 1.14 ppm (d, ^3J(H,H)=6 Hz, 12H); ^{13}C{^{1}H} NMR (75 MHz, [D$_6$]DMSO, 25°C; due to extensive fluorine coupling, coupling constants are not given and resonances are reported as peaks): δ=155.00, 154.62, 151.33, 151.08, 150.70, 143.35, 142.10, 130.43, 130.21, 126.33, 112.72–112.32 (m), 112.14–111.92 (m), 27.89, 25.18 ppm; ^{19}F{^{1}H} NMR (282 MHz, [D$_6$]DMSO, 25°C): δ=−129.06 ppm; HRMS (FAB$^+$): *m/z* calcd for $C_{17}H_{21}N_2F_2$ [M^+]: 291.1673; found: 291.1672.

1-(2,6-Difluorophenyl)-3-(2,6-diisopropylphenyl)-4,5-dihydroimidazolium chloride (18c): This compound was synthesized analogously to **18a** starting with **17c** (white solid, 98% yield). ^{1}H NMR (300 MHz, [D$_6$]DMSO, 25°C): δ = 9.55 (s, 1H), 7.66–7.41 (m, 6H), 4.72 (t, ^3J(H,H) = 10 Hz, 2H), 4.43 (t, ^3J(H,H) = 10 Hz, 2H), 3.05 (septet, ^3J(H,H) = 7 Hz, 2H), 1.29 (d, ^3J(H,H) = 7 Hz, 6H), 1.20 ppm (d, ^3J(H,H) = 7 Hz, 6H); ^{13}C{^{1}H} NMR (75 MHz, [D$_6$]DMSO, 25°C; due to extensive fluorine coupling, coupling constants are not given and resonances are reported as peaks): δ = 161.44, 158.82, 155.47, 146.68, 142.10, 131.88, 130.54, 125.60, 114.35–113.60 (m), 54.79, 52.21, 28.63, 25.43, 24.29 ppm; ^{19}F{^{1}H} NMR (282 MHz, [D$_6$]DMSO, 25°C): δ = −119.89 ppm; HRMS (FAB$^+$): *m/z* calcd for $C_{21}H_{25}N_2F_2$ [M^+]: 343.1986; found: 343.1987.

[RuCl$_2$\{1-(2,6-difluorophenyl)-3-(2,6-diisopropylphenyl)-4,5-dihydroimidazol-2-ylidene\}(=CH−Ph)(PCy$_3$)] (12): Inside a glove box, **18c** (265 mg, 772 μmol, 1.3 equiv) and KHMDS (140 mg, 772 μmol, 1.3 equiv) were stirred in benzene (30 mL) at room temperature for 80 min. Complex **2** (443 mg, 551 μmol, 1.0 equiv) was added as a solid in one portion, and the reaction flask was taken out of the glove box and stirred under a nitrogen atmosphere at room temperature for 4 h. The solvent was completely removed in vacuo. The residual solid was dissolved in a mixture of hexanes/diethyl ether (3 mL, 5:1) and poured onto a column packed with TSI Scientific silica gel. The desired complex was eluted with hexanes/diethyl ether (5:1) as a brown band. This was concentrated in vacuo, transferred in a glove box, dissolved in the minimum amount of benzene, and lyophilized to afford complex **12** as a brown solid (212 mg, 240 μmol, 44% yield). ^{1}H NMR (500 MHz, CD$_2$Cl$_2$, 25°C): δ = 19.41 (s, 1H-minor), 19.13 (s, 1H-major), 7.52–6.69 (m, 11H-major, 11H-minor), 4.16–3.89 (m, 4H-major, 4H-minor), 2.65–0.90 ppm (m, 47H-major, 47H-minor); ^{13}C{^{1}H} NMR (125 MHz, CD$_2$Cl$_2$, 25°C; due to extensive fluorine coupling and the existence of two rotational isomers, coupling constants are not given and resonances are reported as peaks): δ = 297.11 (major), 294.19 (minor), 223.08, 222.45, 192.43, 162.40, 160.36, 152.06, 151.25, 138.78, 138.15, 136.89, 136.72, 135.32, 134.59, 131.36, 131.29, 131.21, 130.12, 129.98, 129.78, 129.16, 128.67, 128.42, 127.92, 126.66, 112.79, 112.63, 111.90, 111.74, 53.17, 52.16, 35.70, 35.22, 34.00, 33.87. 32.03, 31.90, 31.77, 29.19, 27.96, 27.88, 27.20, 27.11, 26.55, 26.41, 21.06, 20.86, 19.70, 18.32 ppm; ^{31}P{^{1}H} NMR (121 MHz, CD$_2$Cl$_2$, 25°C) δ = 31.59 (s, minor), 27.59 ppm (s, major); ^{19}F{^{1}H} NMR (282 MHz, CD$_2$Cl$_2$, 25°C): δ = −110.26 (s, major), −117.22 ppm (s, minor); HRMS (FAB$^+$): *m/z* calcd for $C_{46}H_{63}N_2F_2Cl_2PRu$ [M^+]: 884.3118; found: 884.3126.

[RuCl$_2$\{1-(2,6-difluorophenyl)-3-(2,6-diisopropylphenyl)-4,5-dihydroimidazol-2-ylidene\}(=CH-*o*-*i*PrO−Ph)] (13): This complex was synthesized and purified analogously to complex **9** starting with **12** (green powder, 85% yield). Crystals suitable for X-ray crystallography were grown at room temperature by slow diffusion of hexanes into a solution of **13** in benzene. ^{1}H NMR (500 MHz, CD$_2$Cl$_2$, 25°C): δ = 16.10 (s, 1H), 7.64 (t, ^3J-(H,H) = 8 Hz, 1H), 7.52–7.48 (m, 2H), 7.43 (d, ^3J(H,H) = 8 Hz, 2H), 7.12 (t, ^3J(H,H) = 8 Hz, 2H), 6.89–6.86 (m, 2H), 4.95 (septet, ^3J(H,H) = 6 Hz, 1H), 4.27–4.15 (m, 4H), 3.26 (septet, ^3J(H,H) = 7 Hz, 2H), 1.34 (d, ^3J-(H,H) = 6 Hz, 6H), 1.28 (d, ^3J(H,H) = 7 Hz, 6H), 0.90 ppm (d, ^3J(H,H) = 7 Hz, 6H); ^{13}C{^{1}H} NMR (125 MHz, CD$_2$Cl$_2$, 25°C; due to extensive fluorine coupling, coupling constants are not given and resonances are reported as peaks): δ = 289.19, 215.68, 162.85, 160.82, 152.74, 148.48, 144.00, 137.47, 131.42, 131.33, 131.26, 130.02, 129.65, 125.16, 122.50, 122.23, 113.12, 112.55, 112.53, 112.40, 112.37, 75.50, 56.28, 51.66, 28.16, 25.70, 23.79, 21.49 ppm; ^{19}F{^{1}H} NMR (282 MHz, CD$_2$Cl$_2$, 25°C): δ = −107.90 ppm; HRMS (FAB$^+$): *m/z* calcd for $C_{31}H_{36}N_2OF_2Cl_2Ru$ [M^+]: 662.1217; found: 662.1195.

General method for the synthesis of chlorodicarbonyl(carbene) rhodium(I) complexes 29, 30, and 32: In a glovebox, the corresponding 4,5-dihydro-imidazolium chloride (500 μmol, 1.0 equiv), along with silver(I) oxide (250 μmol, 0.5 equiv), and 4 Å molecular sieves (170 mg) were suspended in CH$_2$Cl$_2$ (4 mL) in the dark. The reaction mixture was stirred at room temperature for 1.5 h, passed through a short celite pad, and then added to a solution of [{Rh(CO)$_2$Cl}$_2$] (97 mg, 250 μmol, 0.5 equiv) in CH$_2$Cl$_2$ (2 mL). This reaction mixture was stirred for an additional 1.5 h in the dark and then passed through a short celite pad. The solvent was removed in vacuo, and the resulting solid was washed with pentanes (5× 2 mL) and dried under high vacuum to afford the desired complex as a powder. (65–75% isolated yield).

General method for the synthesis of chlorodicarbonyl(carbene) rhodium(I) complexes 31 and 33: Inside a glovebox, the corresponding 4,5-dihydro-imidazolium chloride (500 μmol, 1.0 equiv), along with silver(I) oxide (250 μmol, 0.5 equiv), and 4 Å molecular sieves (170 mg) were suspended in CH$_2$Cl$_2$ (4 mL) in the dark. The reaction mixture was stirred at room temperature for 1.5 h, passed through a short celite pad, and then added to a solution of [{Rh(cod)Cl}$_2$] (123 mg, 250 μmol, 0.5 equiv) in CH$_2$Cl$_2$ (2 mL).The new reaction mixture was stirred for an additional 1.5 h in the dark and then passed through a short celite pad. This solution was taken out of the glove box, and poured onto a column packed with TSI Scientific silica gel. The column was initially flushed with CH$_2$Cl$_2$. The desired [Rh(cod)Cl(NHC)] complex was then eluted with EtOH/CH$_2$Cl$_2$ (2:100) as a yellow band. This was concentrated in vacuo, transferred in a glove box, dissolved in the minimum amount of benzene and lyophilized. The obtained solid was finally washed with pentanes (2× 1 mL) to afford a yellow powder. This complex was then dissolved in a dry and deoxygenated 1:1 THF/toluene mixture (3 mL). CO was bubbled through the reaction mixture for 1 h at room temperature. The solvent was removed in vacuo, and the resulting solid was washed with pentanes (2×2 mL) and dried under high vacuum to afford the desired *cis*-[Rh(CO)$_2$Cl(NHC)] complex as a yellow powder. (48–75% isolated yield, two steps).

Characterization of chlorodicarbonyl\{1-(2,6-difluorophenyl)-3-mesityl-4,5-dihydroimidazol-2-ylidene\}rhodium(I) (29): ^{1}H NMR (300 MHz, CD$_2$Cl$_2$, 25°C): δ = 7.48–7.38 (m, 1H), 7.18–7.01 (m, 4H), 4.22–4.00 (m, 4H), 2.39 (s, 6H), 2.35 ppm (s, 3H); ^{13}C{^{1}H} NMR (125 MHz, CD$_2$Cl$_2$, 25°C; due to extensive fluorine coupling, coupling constants are not given and resonances are reported as peaks): δ = 207.65 (d, ^1J(^{103}Rh,^{13}C) = 42 Hz), 185.42 (d, ^1J(^{103}Rh,^{13}C) = 54 Hz), 182.35 (d, ^1J(^{103}Rh,^{13}C) = 74 Hz), 160.82–160.45 (m), 158.81–158.45 (m), 138.88, 136.01, 136.86, 134.56, 129.94, 129.86, 129.79, 129.43, 129.33, 129.19, 112.33–111.67(m), 51.86, 51.72, 20.72, 18.17, 17.94 ppm; ^{19}F{^{1}H} NMR (282 MHz, CD$_2$Cl$_2$, 25°C): δ = −116.42 ppm; HRMS (FAB$^+$): *m/z* calcd for $C_{20}H_{18}ClF_2O_2N_2Rh$ [M^+]: 494.0080; found: 494.0084.

Characterization of chlorodicarbonyl\{1-(2,4,6-trifluorophenyl)-3-mesityl-4,5-dihydroimidazol-2-ylidene\}rhodium(I) (30): ^{1}H NMR (300 MHz, CD$_2$Cl$_2$, 25°C): δ = 7.01 (s, 2H), 6.91–6.85 (m, 2H), 4.20–4.00 (m, 4H), 2.38 (s, 6H), 2.35 ppm (s, 3H); ^{13}C{^{1}H} NMR (125 MHz, CD$_2$Cl$_2$, 25°C; due to extensive fluorine coupling, coupling constants are not given and resonances are reported as peaks): δ = 208.01 (d, ^1J(^{103}Rh,^{13}C) = 41 Hz), 185.33 (d, ^1J(^{103}Rh,^{13}C) = 53 Hz), 182.30 (d, ^1J(^{103}Rh,^{13}C) = 74 Hz), 163.14–162.90 (m), 161.15–160.54 (m), 158.92–158.67 (m), 138.96, 135.73, 134.42, 109.65, 101.11–100.71 (m), 51.94, 51.67, 20.70, 17.90 ppm; ^{19}F{^{1}H} NMR (282 MHz, CD$_2$Cl$_2$, 25°C): δ = −106.66, −113.07 ppm (brs); HRMS (FAB$^+$): *m/z* calcd for $C_{20}H_{17}ClF_3O_2N_2Rh$ [M^+]: 511.9986; found: 511.9980.

Characterization of chlorodicarbonyl\{1-(2,3,4,5,6-pentafluorophenyl)-3-mesityl-4,5-dihydroimidazol-2-ylidene\}rhodium(I) (31): ^{1}H NMR (300 MHz, CD$_2$Cl$_2$, 25°C): δ = 7.02 (s, 2H), 4.24–4.04 (m, 4H), 2.37 (s, 6H), 2.35 ppm (s, 3H); ^{13}C{^{1}H} NMR (125 MHz, CD$_2$Cl$_2$, 25°C; due to extensive fluorine coupling, coupling constants are not given and resonances are reported as peaks): δ = 208.50 (d, ^1J(^{103}Rh,^{13}C) = 41 Hz), 185.07 (d, ^1J(^{103}Rh,^{13}C) = 54 Hz), 182.04 (d, ^1J(^{103}Rh,^{13}C) = 74 Hz), 146.00–145.75 (m), 143.94–143.78 (m), 142.78–142.35 (m), 140.63–140.39 (m), 139.25, 138.96–138.67 (m), 136.95–136.69 (m), 135.60–135.38 (m), 134.15, 129.45, 129.26, 116.44–115.93 (m), 52.08, 51.60, 20.72, 17.88 ppm; ^{19}F{^{1}H} NMR (282 MHz, CD$_2$Cl$_2$, 25°C): δ = −142.99 (brs), −154.39 to −154.54 (m), −162.63 to −162.76 ppm (m); HRMS (FAB$^+$): *m/z* calcd for $C_{19}H_{15}ClF_5ON_2Rh$ [M^+−CO]: 519.9848; found: 519.9856.

Characterization of chlorodicarbonyl\{1,3-bis(2,6-difluorophenyl)-4,5-dihydroimidazol-2-ylidene\}rhodium(I) (32): ^{1}H NMR (300 MHz, CD$_2$Cl$_2$, 25°C): δ = 7.55–7.43 (m, 2H), 7.19–7.09 (m, 4H), 4.24–4.19 ppm (m, 4H); ^{13}C{^{1}H} NMR (125 MHz, CD$_2$Cl$_2$, 25°C; due to extensive fluorine coupling, coupling constants are not given and resonances are reported as peaks): δ = 210.15 (d, ^1J(^{103}Rh,^{13}C) = 40 Hz), 185.42 (d, ^1J(^{103}Rh,^{13}C) = 54 Hz), 181.75 (d, ^1J(^{103}Rh,^{13}C) = 74 Hz), 160.49, 160.18, 158.47, 158.18,

130.60–130.34 (m), 112.38–112.11 (m), 52.17, 51.77 ppm; $^{19}F\{^1H\}$ NMR (282 MHz, CD_2Cl_2, 25 °C): $\delta = -116.66$ ppm; HRMS (FAB$^+$): m/z calcd for $C_{17}H_{10}ClF_4O_2N_2Rh$ [M^+]: 487.9422; found: 487.9421.

Characterization of chlorodicarbonyl{1-(2,6-difluorophenyl)-3-(2,6-diisopropylphenyl)-4,5-dihydroimidazol-2-ylidene}rhodium(I) (33): ^1H NMR (300 MHz, CD_2Cl_2, 25 °C): $\delta = 7.49$–7.39 (m, 2H), 7.32–7.29 (m, 2H), 7.13–7.07 (m, 2H), 4.22–4.07 (m, 4H), 3.27 (septet, $^3J(H,H) = 7$ Hz, 2H), 1.39 (d, $^3J(H,H) = 7$ Hz, 6H), 1.25 ppm (d, $^3J(H,H) = 7$ Hz, 6H); $^{13}C\{^1H\}$ NMR (125 MHz, CD_2Cl_2, 25 °C; due to extensive fluorine coupling, coupling constants are not given and resonances are reported as peaks): $\delta =$ 208.64 (d, $^1J(^{103}Rh,^{13}C) = 42$ Hz), 185.35 (d, $^1J(^{103}Rh,^{13}C) = 54$ Hz), 182.35 (d, $^1J(^{103}Rh,^{13}C) = 75$ Hz), 160.39, 158.38, 147.12, 134.14, 130.03–129.87 (m), 129.68, 124.47, 112.12, 111.96, 54.75, 51.50, 28.24, 26.37, 23.37 ppm; $^{19}F\{^1H\}$ NMR (282 MHz, CD_2Cl_2, 25 °C): $\delta = -116.40$ ppm; HRMS (FAB$^+$): m/z calcd for $C_{22}H_{24}ClF_2ON_2Rh$ [$M^+ - CO$]: 508.0600; found: 508.0590.

Acknowledgements

This research was supported in part by the National Institutes of Health and by a Marie Curie International Fellowship to G.C.V. within the 6th European Community Framework Program. The authors thank Larry M. Henling and Dr. Michael W. Day for the X-ray crystallographic analyses and Dr. Mona Shahgholi for performing the mass spectrometric analyses. Materia Inc. is acknowledged for providing generous gifts of catalyst **2**.

[1] a) *Olefin Metathesis and Metathesis Polymerization* (Eds.: K. J. Ivin, J. C. Mol), Academic Press, San Diego, **1997**; b) *Handbook of Metathesis* (Ed.: R. H. Grubbs), Wiley-VCH, Weinheim, **2003**.

[2] Representative review articles on the applications of olefin metathesis: a) R. H. Grubbs, S. J. Miller, G. C. Fu, *Acc. Chem. Res.* **1995**, *28*, 446–452; b) M. Schuster, S. Blechert, *Angew. Chem.* **1997**, *109*, 2124–2144; *Angew. Chem. Int. Ed. Engl.* **1997**, *36*, 2036–2056; c) R. H. Grubbs, S. Chang, *Tetrahedron* **1998**, *54*, 4413–4450; d) S. K. Armstrong, *J. Chem. Soc. Perkin Trans. 1* **1998**, 371–388; e) K. J. Ivin, *J. Mol. Catal. A* **1998**, *133*, 1–16; f) M. R. Buchmeiser, *Chem. Rev.* **2000**, *100*, 1565–1604; g) A. Fürstner, *Angew. Chem.* **2000**, *112*, 3140–3172; *Angew. Chem. Int. Ed.* **2000**, *39*, 3012–3043; h) T. M. Trnka, R. H. Grubbs, *Acc. Chem. Res.* **2001**, *34*, 18–29; i) S. J. Connon, S. Blechert, *Angew. Chem.* **2003**, *115*, 1944–1968; *Angew. Chem. Int. Ed.* **2003**, *42*, 1900–1923; j) R. R. Schrock, A. H. Hoveyda, *Angew. Chem.* **2003**, *115*, 4740–4782; *Angew. Chem. Int. Ed.* **2003**, *42*, 4592–4633; k) R. H. Grubbs, *Tetrahedron* **2004**, *60*, 7117–7140; l) T. J. Donohoe, A. J. Orr, M. Bingham, *Angew. Chem.* **2006**, *118*, 2730–2736; *Angew. Chem. Int. Ed.* **2006**, *45*, 2664–2670.

[3] S. T. Nguyen, L. K. Johnson, R. H. Grubbs, J. W. Ziller, *J. Am. Chem. Soc.* **1992**, *114*, 3974–3975.

[4] a) P. Schwab, M. B. France, J. W. Ziller, R. H. Grubbs, *Angew. Chem.* **1995**, *107*, 2179–2181; *Angew. Chem. Int. Ed. Engl.* **1995**, *34*, 2039–2041; b) P. Schwab, R. H. Grubbs, J. W. Ziller, *J. Am. Chem. Soc.* **1996**, *118*, 100–110.

[5] M. Scholl, S. Ding, C. W. Lee, R. H. Grubbs, *Org. Lett.* **1999**, *1*, 953–956.

[6] a) J. S. Kingsbury, J. P. A. Harrity, P. J. Bonitatebus, Jr., A. H. Hoveyda, *J. Am. Chem. Soc.* **1999**, *121*, 791–799; b) S. B. Garber, J. S. Kingsbury, B. L. Gray, A. H. Hoveyda, *J. Am. Chem. Soc.* **2000**, *122*, 8168–8179; c) H. Wakamatsu, S. Blechert, *Angew. Chem.* **2002**, *114*, 2509–2511; *Angew. Chem. Int. Ed.* **2002**, *41*, 2403–2405; d) K. Grela, S. Harutyunyan, A. Michrowska, *Angew. Chem.* **2002**, *114*, 4210–4212; *Angew. Chem. Int. Ed.* **2002**, *41*, 4038–4040; e) A. Michrowska, R. Bujok, S. Harutyunyan, V. Sashuk, G. Dolgonos, K. Grela, *J. Am. Chem. Soc.* **2004**, *126*, 9318–9325; f) A. Hejl, M. W. Day, R. H. Grubbs, *Organometallics* **2006**, *25*, 6149–6154.

[7] a) T. J. Seiders, D. W. Ward, R. H. Grubbs, *Org. Lett.* **2001**, *3*, 3225–3228; b) J. J. Van Veldhuizen, S. B. Garber, J. S. Kingsbury, A. H. Hoveyda, *J. Am. Chem. Soc.* **2002**, *124*, 4954–4955; c) J. J. Van Veldhuizen, D. G. Gillingham, S. B. Garber, O. Kataoka, A. H. Hoveyda, *J. Am. Chem. Soc.* **2003**, *125*, 12502–12508; d) D. G. Gillingham, O. Kataoka, S. B. Garber, A. H. Hoveyda, *J. Am. Chem. Soc.* **2004**, *126*, 12288–12290; e) J. J. Van Veldhuizen, J. E. Campbell, R. E. Giudici, A. H. Hoveyda, *J. Am. Chem. Soc.* **2005**, *127*, 6877–6882; f) T. W. Funk, J. M. Berlin, R. H. Grubbs, *J. Am. Chem. Soc.* **2006**, *128*, 1840–1846; g) J. M. Berlin, J. M. Goldberg, R. H. Grubbs, *Angew. Chem.* **2006**, *118*, 7753–7757; *Angew. Chem. Int. Ed.* **2006**, *45*, 7591–7595; h) R. E. Giudici, A. H. Hoveyda, *J. Am. Chem. Soc.* **2007**, *129*, 3824–3825.

[8] a) D. M. Lynn, B. Mohr, R. H. Grubbs, L. M. Henling, M. W. Day, *J. Am. Chem. Soc.* **2000**, *122*, 6601–6609; b) D. M. Lynn, R. H. Grubbs, *J. Am. Chem. Soc.* **2001**, *123*, 3187–3193; c) T. Rölle, R. H. Grubbs, *Chem. Commun.* **2002**, 1070–1071; d) J. P. Gallivan, J. P. Jordan, R. H. Grubbs, *Tetrahedron Lett.* **2005**, *46*, 2577–2580; e) S. H. Hong, R. H. Grubbs, *J. Am. Chem. Soc.* **2006**, *128*, 3508–3509; f) M. T. Mwangi, M. B. Runge, M. B. Bowden, *J. Am. Chem. Soc.* **2006**, *128*, 14434–14435; g) J. B. Binder, I. A. Guzei, R. T. Raines, *Adv. Synth. Catal.* **2007**, *349*, 395–404.

[9] a) J. M. Berlin, K. Campbell, T. Ritter, T. W. Funk, A. Chlenov, R. H. Grubbs, *Org. Lett.* **2007**, *9*, 1339–1342; b) I. C. Stewart, T. Ung, A. A. Pletnev, J. M. Berlin, R. H. Grubbs, Y. Schrodi, *Org. Lett.* **2007**, *9*, 1589–1592.

[10] A. Fürstner, L. Ackermann, B. Gabor, R. Goddard, C. W. Lehmann, R. Mynott, F. Stelzer, O. R. Thiel, *Chem. Eur. J.* **2001**, *7*, 3236–3253.

[11] M. B. Dinger, P. Nieczypor, J. C. Mol, *Organometallics*, **2003**, *22*, 5291–5296.

[12] K. Vehlow, S. Maechling, S. Blechert, *Organometallics* **2006**, *25*, 25–28.

[13] N. Ledoux, B. Allaert, S. Pattyn, H. V. Mierde, C. Vercaemst, F. Verpoort, *Chem. Eur. J.* **2006**, *12*, 4654–4661.

[14] N. Ledoux, B. Allaert, A. Linden, P. Van Der Voort, F. Verpoort, *Organometallics* **2007**, *26*, 1052–1056.

[15] G. C. Vougioukalakis, R. H. Grubbs, *Organometallics* **2007**, *26*, 2469–2472.

[16] N. Ledoux, A. Linden, B. Allaert, H. V. Mierde, F. Verpoort, *Adv. Synth. Catal.* **2007**, *349*, 1692–1700.

[17] P. A. Fournier, S. K. Collins, *Organometallics* **2007**, *26*, 2945–2949.

[18] D. R. Anderson, V. Lavallo, D. J. O'Leary, G. Bertrand, R. H. Grubbs, *Angew. Chem.* **2007**, *119*, 7400–7403; *Angew. Chem. Int. Ed.* **2007**, *46*, 7262–7265.

[19] G. C. Vougioukalakis, R. H. Grubbs, *J. Am. Chem. Soc.* **2008**, *130*, 2234–2245.

[20] A. W. Waltman, R. H. Grubbs, *Organometallics*, **2004**, *23*, 3105–3107.

[21] Comparison of the ^1H NMR chemical shifts in the two rotational isomers of **6**, **8** and **10** with that in parent complex **3** suggests that the major rotational isomer in these unsymmetrical complexes contains a mesityl ring located above the benzylidene moiety. This was confirmed for complexes **6** and **8** by acquiring low-temperature ^1H NMR spectra (−70 °C, CD_2Cl_2) of the crystals studied by X-ray crystallography, which showed only the rotational isomer that has its mesityl ring located directly above the benzylidene group. These spectra showed a ≈5:95 ratio for the two benzylidene protons, as compared to the room temperature ratio of ≈2:8. Unfortunately, it was not possible to obtain any diagnostic information regarding this issue from NOE experiments in solution.

[22] For two review articles on π–π stacking interactions, see: a) J. H. Williams, *Acc. Chem. Res.* **1993**, *26*, 593–598; b) C. Janiak, *J. Chem. Soc. Dalton Trans.* **2000**, 3885–3896; for two recent publications on intramolecular π–π stacking interactions see: c) D. Mandal, B. D. Gupta, *Organometallics*, **2006**, *25*, 3305–3307; d) D. Mandal, B. D. Gupta, *Organometallics*, **2007**, *26*, 658–670.

[23] Low-quality crystals of complex **11** were also obtained. X-ray analysis on different samples of these single crystals showed the same connectivity and orientation of the ligands as in the crystal structures of the complexes **8**, **9**, and **13**.

[24] For a comparative catalytic evaluation study of the most commonly-used ruthenium-based olefin metathesis catalysts, see: T. Ritter, A. Hejl, A. G. Wenzel, T. W. Funk, R. H. Grubbs, *Organometallics* **2006**, *25*, 5740–5745.
[25] C. Slugovc, *Macromol. Rapid Commun.* **2004**, *25*, 1283–1297.
[26] A. K. Chatterjee, T. L. Choi, D. P. Sanders, R. H. Grubbs, *J. Am. Chem. Soc.* **2003**, *125*, 11360–11370.
[27] J. Louie, R. H. Grubbs, *Organometallics* **2002**, *21*, 2153–2164.
[28] a) M. S. Sanford, M. Ulman, R. H. Grubbs, *J. Am. Chem. Soc.* **2001**, *123*, 749–750; b) M. S. Sanford, J. A. Love, R. H. Grubbs, *J. Am. Chem. Soc.* **2001**, *123*, 6543–6554; according to these studies, the higher activity of the second- versus the first-generation ruthenium-based metathesis catalysts originates from the increased affinity of the NHC-substituted ruthenium center for π-acidic olefins relative to σ-donating phosphine, and not from the increased labilization of the phosphine due to the large *trans*-effect of the NHC ligands, as originally believed.
[29] A. H. Hejl, Ph.D. thesis, California Institute of Technology (USA), **2007**.
[30] The kinetics in the initiation of the phosphine-free catalysts are much more complicated than for the phosphine-containing ones. Detailed studies designed to fully understand the initiation mechanism of olefin metathesis catalysts with chelating alkylidenes are currently underway and will be published in due course.
[31] a) K. Denk, P. Sirsch, W. A. Herrmann, *J. Organomet. Chem.* **2002**, *649*, 219–224; b) M. Mayr, K. Wurst, K. H. Ongania, M. R. Buchmeiser, *Chem. Eur. J.* **2004**, *10*, 1256–1266; c) W. A. Herrmann, J. Schütz, G. D. Frey, E. Herdtweck, *Organometallics* **2006**, *25*, 2437–2448.
[32] For two ruthenium-based metathesis catalysts coordinated with this NHC, see: T. Ritter, M. W. Day, R. H. Grubbs, *J. Am. Chem. Soc.* **2006**, *128*, 11768–11769.
[33] For a cyclic voltametry study on the π-face donor properties of NHCs in some related ruthenium-based metathesis catalysts, see: a) M. Süßner, H. Plenio, *Chem. Commun.* **2005**, 5417–5419; see also: b) S. Leuthäußer, D. Schwarz, H. Plenio, *Chem. Eur. J.* **2007**, *13*, 7195–7203.
[34] A. B. Pangborn, M. A. Giardello, R. H. Grubbs, R. K. Rosen, F. J. Timmers, *Organometallics* **1996**, *15*, 1518–1520.

Received: March 13, 2008
Published online: July 21, 2008

Please note: Minor changes have been made to this Manuscript since its publication in Chemistry—A European Journal Early View. The Editor.

